Copy
RM E52A14

NACA

RESEARCH MEMORANDUM

DYNAMIC RESPONSE OF TURBINE-BLADE TEMPERATURE TO EXHAUST-GAS TEMPERATURE FOR GAS-TURBINE ENGINES

By Richard Hood and William E. Phillips, Jr.

Lewis Flight Propulsion Laboratory
Cleveland, Ohio

NATIONAL ADVISORY COMMITTEE
FOR AERONAUTICS

WASHINGTON
February 20, 1952

NATIONAL ADVISORY COMMITTEE FOR AERONAUTICS

RESEARCH MEMORANDUM

DYNAMIC RESPONSE OF TURBINE-BLADE TEMPERATURE TO EXHAUST-GAS TEMPERATURE FOR GAS-TURBINE ENGINES

By Richard Hood and William E. Phillips, Jr.

SUMMARY

The frequency response of blade temperature to exhaust-gas temperature for two locations in the blade and several operating conditions determined from harmonic analysis of transient data is presented. Two analytical methods are compared with the experimental frequency response of the blade temperature to the gas temperature. The dynamic response of turbine-blade temperature to exhaust-gas temperature exhibited the form of a first-order lag. The time constant of the lag for the leading-edge position of the turbine blade was found to be approximately 6.6 seconds. The time constant of the lag for the midchord position of the turbine blade was found to be three times that of the leading-edge position.

These results were used to predict blade temperature for typical controlled and uncontrolled gas-turbine engines.

INTRODUCTION

In general, gas-turbine engines are regulated through the measured values of engine speed and turbine exhaust-gas temperature. This regulation has the two-fold purpose of controlling engine performance and minimizing engine damage. Exhaust-gas temperature may cause engine damage by affecting blade temperature. Present practice limits exhaust-gas temperature to some level which is considered safe for turbine-blade life. This temperature limitation imposes severe restrictions on acceleration rates of the engine. Use of heat transfer theory shows that during transients the blade temperature will not correspond to the exhaust-gas temperature and that this dynamic characteristic could result in a relaxed restriction on exhaust-gas temperature during transients.

An investigation of the dynamic response of turbine-blade temperature to exhaust-gas temperature for a gas-turbine engine was made at the NACA Lewis laboratory. For this investigation, a gas-turbine engine was

instrumented so that simultaneous recordings of exhaust-gas temperature and turbine-blade temperature were obtained during various transient and acceleration conditions. The results of these experiments and their application to gas-turbine engine operation and control are presented herein and several examples of the application of the results obtained are cited. The general relation of turbine-blade temperature to exhaust-gas temperature as defined by heat-transfer theory is also presented. The comparison of the analytical and the experimental relation is discussed.

ANALYSIS

Two methods of determining the dynamic response of turbine-blade temperature to exhaust-gas temperature are presented. Method A considers only the lag due to the film coefficient and method B also considers the temperature gradient in the blade.

These two methods of determining the dynamic response of turbine-blade temperature to gas temperature involve the physical properties of the blade material, the temperatures of the blade and the gas, and the attendant film coefficient. A method of determining the appropriate film coefficient is presented in reference 1.

Analytical Method A

Method A assumes that the temperature is equal throughout the blade and that the heat flow is proportional to the difference in temperature between the gas and the blade. The heat flow from the gas to the blade is also assumed to be utilized completely in raising the blade temperatures. This relation can be expressed mathematically as:

$$\frac{dq}{dt} = h A (T_g - T_b) \tag{1}$$

$$\frac{dq}{dt} = V \rho c_p \frac{dT_b}{dt} \tag{2}$$

(All symbols are defined in appendix A.)

Combining equations (1) and (2) gives the general form of the dynamic response of blade temperature to gas temperature as:

$$\frac{V\rho c_p}{hA} \frac{dT_b}{dt} + T_b = T_g \tag{3}$$

As equation (3) is a first-order differential equation, it can be characterized by a time constant τ_b, which is defined as:

$$\tau_b \triangleq \frac{V\rho c_p}{hA}$$

and has the units of time. The time constant is therefore based on the physical properties and dimensions of the blade and the heat-transfer film coefficient.

Equation (3) may be converted from the time domain to the frequency domain by Laplacian transformation methods discussed in reference 2, chapter 3. This conversion gives a transfer function (the ratio of the blade temperature to the gas temperature) of the form:

$$\frac{T_b}{T_g} = \frac{1}{1+i\omega\tau_b} \tag{4}$$

where τ_b has already been defined. The amplitude and phase of equation (4) as a function of frequency ω are plotted on logarithmic coordinates (fig. 1). This method is discussed in reference 2, chapter 8. The asymptotes to the curve of figure 1 intersect at a frequency of one radian per second. Because the time constant is the reciprocal of this intersecting frequency, τ_b is also unity, which was the value chosen for the curve. This method of obtaining the intersection of the asymptotes was used throughout the report to determine the time constants from the plots of the experimental data.

Analytical Method B

A more inclusive method of determining the dynamic response of turbine-blade temperature to gas temperature is developed by means of the heat-transfer equation

$$\alpha^2\nabla^2 T = \frac{\partial T}{\partial t} \tag{5}$$

and appropriate boundary conditions.

Leading-edge blade temperature. - The dynamic response of the leading-edge blade temperature to gas temperature can be determined by equation (5) and appropriate boundary conditions. The frequency response of leading-edge blade temperature to gas temperature is

$$\frac{T_b}{T_g \text{ at } r=0} = \frac{1}{J_0\left(i^{3/2}\frac{\sqrt{\omega}}{\alpha}R\right) - \frac{i^{3/2}\sqrt{\omega}}{\alpha K}J_1\left(i^{3/2}\frac{\sqrt{\omega}}{\alpha}R\right)} \qquad (6)$$

The derivation of equation (6) and the attendant assumptions are given in appendix B. A plot of equation (6) in figure 2(a) presents the amplitude and phase of the frequency response of the leading-edge blade temperature to the gas temperature.

Midchord blade temperature. - The dynamic response of midchord blade temperature to gas temperature can be determined by equation (5) and suitable boundary equations. The frequency response of the midchord blade temperature developed in appendix B is

$$\frac{T_b}{T_g \text{ at } x=\frac{a}{2}} = \frac{1}{\frac{\sqrt{i\omega}}{\alpha K}\sinh\frac{\sqrt{i\omega}\,a}{2\alpha} + \cosh\frac{\sqrt{i\omega}\,a}{2\alpha}} \qquad (7)$$

The amplitude and phase relations to frequency of equation (7) are presented as figure 2(b).

Trailing-edge blade temperature. - The dynamic response of the trailing-edge blade temperature to gas temperature could be determined in the same manner as the leading-edge blade temperature response; however, the difficulty of accurately determining the film coefficient at the trailing-edge position makes this evaluation impractical.

APPARATUS AND PROCEDURE

Test Engine

The turbojet engine from which the data were obtained has a centrifugal-type compressor and a single-stage turbine. This engine was operated over the power range (idle to full power) at sea-level conditions. A schematic drawing of the turbojet engine showing the

locations of the stations at which the temperature was measured appears in figure 3. Station 1 is in the turbine rotor blades and station 2 is in the tail cone approximately 3 to 4 feet downstream of the turbine.

Temperature Measurement Methods

The temperatures were indicated by thermocouples and recorded by a galvanometric oscillograph. The frequency responses of the oscillograph galvanometric elements were such that no correction was necessary to the traces for the frequency range of the experimental data.

Blade temperature. - The blade temperature was indicated by a 36-gage chromel-alumel wire thermocouple imbedded in the airfoil section of the blade. The thermocouple junction was peened to the blade material. The emf of the blade thermocouples was transferred through slip rings at the front of the engine from the rotating shaft and then through bucking circuits to the oscillograph.

The leading-edge-position blade thermocouple was located in the turbine blade as illustrated in figure 4(a). The spanwise position of the thermocouple, approximately at the midpoint of the airfoil section, was chosen as the most critical section of the blade because of the combined effects of centrifugal stress and temperature.

The midchord-position blade thermocouple was located at approximately the same spanwise position as the leading-edge thermocouple. As the blade was structurally weakened by the insertion of the thermocouple, the tip of the blade was removed so that the blade would be able to withstand the stresses of full-power operation of the engine. The turbine blade used is shown in figure 4(b).

The trailing-edge position of the turbine blade was not tested. For certain classes of materials used in turbine blades, unpublished work indicates that the failures due to temperature are almost entirely limited to the leading-edge and midchord positions. The trailing-edge position failures are attributed to vibratory stress.

Gas temperature. - The gas temperature was indicated by four 28-gage chromel-alumel thermocouples placed at station 2 shown in figure 3. The emf generated by the thermocouples passed through a bucking circuit and then to the oscillograph. The time constant of these thermocouples was approximately 0.15 second for the particular installation; therefore the gas temperature traces were not corrected for the gas thermocouple lag, which was too small to have significant effect on the data.

Analysis of Data

Method of data reduction. - The data recorded by the galvanometric oscillograph were in the form of figure 5. These traces, which are the temperatures of the gas and blade recorded against time, were reduced by harmonic analysis so as to obtain separately the frequency response of the blade temperature and the gas temperature to the same arbitrary fuel-flow input. The ratio of these two frequency responses is the frequency response of turbine-blade temperature to gas temperature.

The harmonic analysis was performed for 34 frequencies by digital computers following the method of reference 3. The frequency response of the traces of figure 5 is presented in figure 6.

RESULTS AND DISCUSSION

Experimental Data

Typical oscillograph traces of temperature of the blade and the gas temperature are presented as figures 5, 7, and 8. The ordinate of the figures is temperature as a deviation from initial value of the trace. The abscissa is time in 0.1-second intervals. The 1-second intervals are so marked. These three figures illustrate the three basic methods by which the experimental data were obtained. In the first method, illustrated by figure 5, the data were obtained by a rapid advance of the fuel flow. The gas temperature first overshot and then went below the final value before reaching the final value. The blade temperature slowly approached the final value. In the second method, illustrated by figure 7, the data were obtained by a sudden decrease in fuel flow to the engine. The gas temperature dropped much lower than the final temperature and then increased. The increase was due mainly to the decrease in air flow attendant to the decrease in speed. The blade temperature decreased very slowly to the final blade temperature. The third basic method illustrated by figure 8 was a combination of the first two methods. The sudden increase in fuel flow was followed by a sudden decrease in fuel flow back to the initial fuel flow. It was intended that the blade temperature would not reach equilibrium at the higher fuel flow thereby establishing a measure of the linearity of the system.

Leading-edge blade temperature. - Typical oscillograph traces of leading-edge blade temperature and gas temperature are shown in figures 5 and 8.

The frequency response of the leading-edge blade temperature to gas temperature for the time traces of figure 5 is given by figure 6.

The curve of figure 6 can be closely approximated by a single first-order lag:

$$\frac{T_b}{T_g} = \frac{1}{1 + i\tau_b\omega} \tag{8}$$

The time constant τ_b is found from the intersection of the asymptotes of the upper or amplitude curve. The asymptotes of figure 6 intersect at a frequency of 0.154 radian per second. The time constant which is the reciprocal of the frequency, is 6.5 seconds. For a step change in gas temperature, the blade temperature will attain 98 percent of its final value in four time constants or 26 seconds.

The lower or phase curve of figure 6 is the phase of the blade temperature with respect to the gas temperature. The phase curve also exhibits the form of a first-order lag system.

The frequency response of leading-edge blade temperature to gas temperature when the fuel flow is decreased suddenly is shown in figure 9. The amplitude and phase curves indicate that the system is predominantly first order and that the time constant τ_b is equal to 7.2 seconds.

The frequency response corresponding to the oscillographic traces of figure 8 is shown in figure 10. The amplitude and phase curves exhibit the form of a first-order lag with a time constant of 6.7 seconds.

Midchord blade temperature. - Typical oscillograph traces of midchord blade temperature and gas temperature are shown in figure 7. The frequency response of midchord blade temperature to gas temperature for the data presented in figure 7 is presented in figure 11. The amplitude relation to frequency exhibits a first-order lag with a time constant of 20.8 seconds. The phase-frequency relation exhibits a first-order lag except for the higher frequencies. The measurement of blade temperature will not, in general, be in a closed loop control so the amplitude relation is the important factor.

The frequency response of midchord blade temperature to gas temperature when the fuel flow is increased is presented as figure 12. The amplitude-frequency relation shows a first-order system with a time constant of 30 seconds. The phase-frequency relation exhibits the general first-order lag form.

Comparison of Analytical and Experimental Data

The comparison of the results of the two analytical methods with the experimental data shows reasonable correlation between the time constants of the first-order approximation of each method. The phase angle results, however, are more varied in their predictions. The experimental and analytical time constants obtained are tabulated as follows:

	Transient	Position	
		Leading edge	Midchord
Experimental data	Acceleration	6.4 6.5	30
	Deceleration	7.2	20.8
	Acceleration, deceleration	6.7 7.2	
Analytical method A		6.8	17.7
Analytical method B		6.3	20.7

Leading-edge blade temperature. - A comparison of the frequency response obtained by the two analytical methods and the representative experimental data for the leading-edge blade temperature to gas temperature is presented as figure 13(a). The application of the heat-transfer equation (equation (5)) gave results very close to the experimental values for the amplitude relation, while analytical method A gave a slightly higher time constant than the experimental. The results of both analytical methods are close enough to use the simple method for analytical studies of the leading-edge blade temperature during a transient. The phase relation (the lower curve) shows more scatter but the accuracy in the phase plane is not as important as the amplitude relation unless the blade temperature is used as part of a closed loop control.

Midchord blade temperature. - A comparison of the frequency responses by the two analytical methods and the experimental data for the midchord blade temperature to gas temperature is presented as figure 13(b). The results for the frequency response at the midchord section of the blade show more deviation. However, both analytical methods are on the conservative side. The phase relation (the lower curve) indicates that the disagreement could be due to nonlinearities in the actual blade that were not accounted for by the analytical methods. This disagreement, however, has a pronounced effect only at a frequency such that the amplitude ratio is quite small and thereby does not appreciably affect the validity of the linear first-order approximation if the relation is not used as part of a closed loop control.

APPLICATION

Effect of Blade-Temperature Lag on Uncontrolled Engine Operation

For present day engines, the engine speed lags the gas temperature (reference 4) which is stated mathematically as

$$\frac{N}{T_g} = B \frac{1}{1 + \tau p} \tag{9}$$

and according to this present report blade temperature lags the gas temperature equation (8). The relation between engine speed and blade temperatures has the form

$$\frac{T_b}{N} = B \frac{1 + \tau p}{1 + \tau_b p} \tag{10}$$

In appendix B it is proved that if τ_b is greater than τ, the turbine-blade temperature will never reach a temperature higher than the final steady-state temperature as long as the final speed is always greater than the engine speed during the transient. Conversely, if τ is greater than τ_b, the turbine-blade temperatures will be higher than the final blade temperature during an acceleration even if the engine speed is everywhere less than the final speed during the transient.

The case where τ_b is greater than τ is shown in figure 14. Gas temperature initially was three times the final gas temperature and the fuel flow was twice the final fuel flow. This condition resulted in rapid acceleration of the engine while the blade temperature rose more slowly. When the engine speed reached the final value, engine fuel flow was changed to the steady-state fuel flow for the speed whereupon the gas temperature also changed to the final gas temperature. For practical purposes, the engine was then in steady-state operation; however, the blade temperature had reached only 35 percent of its final value.

The relations which result during a transient when the blade temperature to gas temperature time constant τ_b is less than the engine speed to gas temperature time constant τ are illustrated in figure 15. The fuel flow and gas temperature transients were assumed the same as for figure 14 which would result in the same speed curve. However, the blade temperature, which leads the engine speed, overshoots the final value before the engine speed has reached the final value. A higher speed cannot be reached with this configuration without exceeding the final blade temperature during the transient.

Effect of Blade-Temperature Lag on Controlled

Engine Operation

The application of the blade-temperature time constant to a closed loop speed control system is shown in figure 16. A block diagram with the various gain constants and time constants and the time responses of speed, gas temperature, and blade temperature to a step increase in set speed are shown. The engine gain constant, which for simplification contains the controller gain also, and the controller integral time constant were chosen to give a damping ratio of 0.707 in the speed loop and to give the gas temperature transient an initial slope of zero. The blade temperature to gas temperature time constant was taken as 4 seconds, which is lower than the values obtained from the experimental data for leading-edge and midchord positions.

As shown, for a step change in set speed, the gas temperature had an initial rise of 2.8 and then decreased to steady state as the speed increased. Because the speed loop was underdamped, the speed transient overshot slightly although the blade temperature did not overshoot.

SUMMARY OF RESULTS

The response of turbine-blade temperature to gas temperature can be considered as a first-order lag in control applications. The time constant of the lag of the blade temperature to gas temperature varies with location on or within the blade. Two analytical methods are presented which predict this lag at the various locations. The leading-edge position of the turbine blade had a time constant of approximately 6.6 seconds. The variation of time constants was found to be in the order of 3 to 1 between the midchord position and the leading-edge position of the blade.

The investigation showed that if the blade temperature to gas temperature time constant is greater than the engine speed to gas temperature time constant, the blade temperature will not exceed the final temperature during a transient from an initial speed to a final speed which is higher than the initial speed. Conversely, if the blade temperature time constant is smaller than the engine speed to gas temperature time constant, the blade temperature will always exceed the final blade temperature during an acceleration transient.

Lewis Flight Propulsion Laboratory
National Advisory Committee for Aeronautics
Cleveland, Ohio

APPENDIX A

SYMBOLS

A	surface area of turbine-blade airfoil section, sq in.
a	blade thickness at midchord and midspan, in.
B	constant, rpm/$^{\circ}$R
C_1, C_2	constants of integration
c_p	specific heat of turbine-blade material, $\frac{\text{Btu}}{\text{lb } ^{\circ}\text{F}}$
F	general function in cylindrical coordinates
G	general function in Cartesian coordinates
h	film coefficient, Btu/(sq ft)(hr)($^{\circ}$F) (from reference 1)
i	$\sqrt{-1}$
J_0	Bessel function of first kind and zero order
J_1	Bessel function of first kind and first order
K	proportionality constant, $\frac{h}{k}$, 1/in.
k	conductivity of blade material, Btu in./(sq ft)(hr)($^{\circ}$F)
N	engine speed, rpm
p	differential operator $\frac{d}{dt}$
q	heat, Btu
R	radius of leading edge of turbine blade, in.
r, θ, z	cylindrical coordinates
T	temperature, $^{\circ}$R
t	time, sec
V	volume of airfoil section of turbine blade, cu in.

w_f	engine fuel flow
x, y, z	Cartesian coordinates
Y_0	Bessel function of second kind and zero order
α	diffusivity of turbine-blade material, $\sqrt{\frac{\text{ft in.}}{\text{hr}}}$
ρ	density of turbine-blade material, lb/cu ft
τ	gas-turbine engine time constant response to gas temperature, sec
τ_b	turbine-blade time constant for response to gas temperature, sec
ω	circular frequency, radians/sec

Subscripts:

b	blade
g	gas
s	setting
ε	error

Superscripts:

'	differentiation with respect to argument
.	differentiation with respect to time

APPENDIX B

ANALYTICAL METHOD B

Analytical method B, which uses the heat-transfer equation, takes into account the temperature gradient across the blade thereby giving a more rigorous method of determining the blade-temperature frequency response to gas temperature.

Leading-edge blade temperature. - The heat-flow equation, written in polar coordinates, is

$$\frac{1}{r}\frac{\partial}{\partial r}\left(r\frac{\partial T_b}{\partial r}\right) + \frac{1}{r^2}\frac{\partial^2 T_b}{\partial \theta^2} = \frac{1}{\alpha^2}\frac{\partial T_b}{\partial t} \tag{B1}$$

This equation is two-dimensional and in using it, no heat flow is assumed in the spanwise direction of the blade. The other boundary conditions imposed on the leading-edge position are:

(1) The heat flow in the angular direction is zero:

$$\frac{\partial T_b}{\partial \theta} = 0 \tag{B2}$$

(2) The rate of heat flow through the surface of the blade is proportional to the temperature difference between the blade surface and the gas:

$$\left(\frac{\partial T_b}{\partial r}\right)_{r=R} = K(T_g - T_b)_{r=R} \tag{B3}$$

Since any arbitrary function may be assumed for T_g,

$$T_g = e^{i\omega t}$$

The blade temperature may now be written as:

$$T_b = F(\omega, r, \theta)\ e^{i\omega t}$$

which means that:

$$\frac{\partial T_b}{\partial r} = F_r e^{i\omega t} \tag{B4}$$

and

$$\frac{\partial T_b}{\partial t} = i\omega F e^{i\omega t} \tag{B5}$$

Combining equations (B1), (B2), (B4), and (B5) gives:

$$\frac{1}{r}\frac{\partial}{\partial r}(rF_r) = \frac{i\omega}{\alpha^2} F \tag{B6}$$

Carrying out the partial differentiation indicated gives:

$$\frac{1}{r}\left[F_r + rF_{rr}\right] = \frac{i\omega F}{\alpha^2} \tag{B7}$$

or

$$F_{rr} + \frac{1}{r} F_r - \frac{i\omega}{\alpha^2} F = 0 \tag{B8}$$

Equation (B8) is one form of Bessel's differential equation and the general solution may be written as:

$$F = C_1 J_0\left(\frac{\sqrt{-i\omega}\ r}{\alpha}\right) + C_2 Y_0\left(\frac{\sqrt{-i\omega}\ r}{\alpha}\right) \tag{B9}$$

Since F has a finite value at $r = 0$, and $Y_0 \to \infty$ as $r \to 0$, C_2 must equal zero, giving

$$F = C_1 J_0\left(\frac{\sqrt{-i\omega}\ r}{\alpha}\right) \tag{B10}$$

Substituting in equation (B3) to obtain the value of the constant C_1 gives

$$F_{r\,r=R}\, e^{i\omega t} = K\left[e^{i\omega t} - F(R)e^{i\omega t}\right]$$

or

$$F_{r\,r=R} = K\left[1 - F(R)\right] \tag{B11}$$

Substituting equation (B10) into equation (B11) gives

$$\frac{\sqrt{i\omega}}{\alpha} C_1 J_0'\left(\frac{\sqrt{-i\omega}}{\alpha}R\right) = K - KC_1 J_0\left(\frac{\sqrt{-i\omega}}{\alpha}R\right)$$

$$\therefore C_1 = \frac{K}{\frac{\sqrt{i\omega}}{\alpha} J_0'\left(\frac{\sqrt{-i\omega}}{\alpha}R\right) + KJ_0\left(\frac{\sqrt{-i\omega}}{\alpha}R\right)}$$

since $J_0' = -J_1$

$$C_1 = \frac{1}{J_0\left(\frac{\sqrt{-i\omega}}{\alpha}R\right) - \frac{\sqrt{-i\omega}}{\alpha K} J_1\left(\frac{\sqrt{-i\omega}}{\alpha}R\right)} \tag{B12}$$

Therefore, equation (B10) becomes

$$F = \frac{J_0\left(\frac{\sqrt{-i\omega}}{\alpha}r\right)}{J_0\left(\frac{\sqrt{-i\omega}}{\alpha}R\right) - \frac{\sqrt{-i\omega}}{\alpha K} J_1\left(\frac{\sqrt{-i\omega}}{\alpha}R\right)} \tag{B13}$$

Now at $r = 0$, $J_0\left(\frac{\sqrt{-i\omega}}{\alpha}r\right) = 1$ and equation (B13) is:

$$F_{r=0} = \frac{1}{J_0\left(\frac{\sqrt{-i\omega}}{\alpha}R\right) - \frac{\sqrt{-i\omega}}{\alpha K} J_1\left(\frac{\sqrt{-i\omega}}{\alpha}R\right)} \tag{B14}$$

If this equation is rewritten in a form more easily obtainable from tables:

$$F_{r=0} = \frac{1}{J_0\left(\frac{i^{3/2}\sqrt{\omega}}{\alpha} R\right) - \frac{i^{3/2}\sqrt{\omega}}{\alpha K} J_1\left(\frac{i^{3/2}\sqrt{\omega}}{\alpha} R\right)} \tag{6}$$

Midchord blade temperature. - In this case, a one-dimensional flow pattern is assumed, which gives for the heat-flow equation

$$\frac{\partial^2 T_b}{\partial x^2} = \frac{1}{\alpha^2}\frac{\partial T_b}{\partial t} \tag{B15}$$

which means that

$$\frac{\partial T_b}{\partial y} = \frac{\partial T_b}{\partial z} = 0$$

Reference to figure 17 gives the boundary conditions as:

$$\frac{\partial T_b}{\partial x}(0,t) = K\left[T_b(0,t) - T_g\right] \tag{B16}$$

$$\frac{\partial T_b}{\partial x}(a,t) = -K\left[T_b(a,t) - T_g\right] \tag{B17}$$

Now, the transfer function G between blade temperature T and gas temperature T_g is assumed to be of the form:

$$G = C_1 e^{rx} + C_2 e^{-rx} \tag{B18}$$

and since T_g may be any arbitrary function, if

$$T_g = e^{i\omega t} \tag{B19}$$

$$T = Ge^{i\omega t} \tag{B20}$$

Substituting equation (B20) into equations (B15), (B16), and (B17) gives

$$G_{xx} = \frac{i\omega}{\alpha^2} G \tag{B21}$$

$$G_x(0) = K\left[G(0) - 1\right] \tag{B22}$$

$$G_x(a) = - K\left[G(a) - 1\right] \tag{B23}$$

Combining equation (B18) with equations (B22) and (B23) yields

$$rC_1e^{rx} - rC_2e^{-rx} = K\left[C_1e^{rx} + C_2e^{-rx} - 1\right] \tag{B24}$$

and

$$rC_1e^{rx} - rC_2e^{-rx} = - K\left[C_1e^{rx} + C_2e^{-rx} - 1\right] \tag{B25}$$

Since $x = 0$ in (B24), it becomes

$$rC_1 - rC_2 = K\left[C_1 + C_2 - 1\right] \tag{B26}$$

and since $x = a$ in (B25), it becomes

$$rC_1e^{ra} - rC_2e^{-ra} = - K\left[C_1e^{ra} + C_2e^{-ra} - 1\right] \tag{B27}$$

Equation (B26) is solved for C_1

$$C_1 = \frac{C_2\,(K + r) - K}{r - K} \tag{B28}$$

And solving equation (B27) for C_2 yields:

$$C_2 = \frac{C_1 e^{ra}(r+K) - K}{(r-K)e^{-ra}} \tag{B29}$$

Substituting equation (B28) into equation (B29) gives:

$$C_2 = \left[\frac{C_2(K+r) - K}{(r-K)^2}\right](K+r)e^{2ra} - \frac{Ke^{ra}}{(r-K)} \tag{B30}$$

And solving equation (B30) for C_2 gives

$$C_2 = \frac{Ke^{ra}}{(K+r)e^{ra} - (r-K)} \tag{B31}$$

Substituting (B31) back into (B28) gives for C_1

$$C_1 = \frac{K(K+r)e^{ra}}{(r^2-K^2)e^{ra} - (r-K)^2} - \frac{K}{r-K} \tag{B32}$$

Substituting the values for C_1 and C_2 from equations (B31) and (B32) into equation (B18) results in

$$G = \left[\frac{K(K+r)e^{ra}}{(r^2-K^2)e^{ra} - (r-K)^2} - \frac{K}{r-K}\right]e^{rx} + \left[\frac{Ke^{ra}}{(K+r)e^{ra} - (r-K)}\right]e^{-rx} \tag{B33}$$

Equation (B33) can be simplified to

$$G = \frac{K\left[e^{-r\left(x-\frac{a}{2}\right)} + e^{r\left(x-\frac{a}{2}\right)}\right]}{e^{\frac{ra}{2}}(K+r) - (r-K)e^{\frac{ra}{2}}} \tag{B34}$$

which in turn becomes

$$G = \frac{\cosh\left[r\left(x - \frac{a}{2}\right)\right]}{\frac{r}{K}\sinh\left(\frac{ra}{2}\right) + \cosh\frac{ra}{2}} \tag{B35}$$

Now substituting equation (B18) into equation (B21) to obtain r gives

$$r^2C_1e^{rx} + r^2C_2e^{-rx} = \frac{i\omega}{\alpha^2}\left(C_1e^{rx} + C_2e^{-rx}\right) \tag{B36}$$

From equation (B36)

$$r = \frac{\sqrt{i\omega}}{\alpha} \tag{B37}$$

and equation (B35) becomes

$$G = \frac{1}{\frac{\sqrt{i\omega}}{\alpha K}\sinh\left(\frac{\sqrt{i\omega}}{\alpha}\frac{a}{2}\right) + \cosh\left(\frac{\sqrt{i\omega}}{\alpha}\frac{a}{2}\right)} \tag{7}$$

where $x = \frac{a}{2}$.

Effect of Blade-Temperature Lag on Uncontrolled Engine Operation

The proof of the statement on ratio of time constants follows herein:

The relation between the engine speed and the turbine blade temperature is

$$\frac{T_b}{N} = B\,\frac{1+\tau p}{1+\tau_b p} \tag{10}$$

which is rewritten and p replaced by $\frac{d}{dt}$

$$\tau_b \frac{dT_b}{dt} + T_b = B\tau \frac{dN}{dt} + BN \tag{B38}$$

the left side is rewritten

$$\tau_b e^{-t/\tau_b} \frac{d}{dt}\left(e^{t/\tau_b} T_b\right) = B\tau \frac{dN}{dt} + BN \tag{B39}$$

Transposing and integrating yields

$$e^{t/\tau_b} T_b \Big|_0^{t_1} = \frac{B\tau}{\tau_b} \int_0^{t_1} e^{t/\tau_b} \dot{N}\, dt + \frac{B}{\tau_b} \int_0^{t_1} e^{t/\tau_b} N\, dt \tag{B40}$$

$$e^{t_1/\tau_b} T_b(t_1) - T_b(0) = \frac{B\tau}{\tau_b} e^{t_1/\tau_b} N(t_1) - \frac{B\tau}{\tau_b} N(0) + \left(1 - \frac{\tau}{\tau_b}\right) \int_0^{t_1} e^{t/\tau_b} N \frac{dt}{\tau_b} \tag{B41}$$

If the engine were in steady state operation at the initial time $t = 0$ then

$$T_b(0) = BN(0) \tag{B42}$$

and the amount that blade temperature is off the steady-state value for any value of speed can be represented by X

$$T_b(t) = BN(t) - X(t) \tag{B43}$$

Substituting equations (B42) and (B43) in equation (B41) gives

$$\frac{X(t_1)}{\left(1 - \frac{\tau}{\tau_b}\right)} = \left[BN(t_1) - e^{-t_1/\tau_b}\, BN(0)\right] - \int_0^{t_1} e^{t-t_1/\tau_b}\, BN(t)\, \frac{dt}{\tau_b} \tag{B44}$$

The right-hand side of equation (B44) can be shown to be positive at all times under certain restrictions on transients.

$$BN(t_1) - e^{-t_1/\tau_b}\, BN(0) \gtrless \int_0^{t_1} e^{t-t_1/\tau_b}\, BN(t)\, \frac{dt}{\tau_b} \tag{B45}$$

Subtracting $\int_0^{t_1} BN(t_1)\, e^{t-t_1/\tau_b}\, \frac{dt}{\tau_b}$ from both sides yields

$$e^{-t_1/\tau_b}\left[BN(t_1) - BN(0)\right] \gtrless \int_0^{t_1} e^{t-t_1/\tau_b}\left[BN(t) - BN(t_1)\right]\frac{dt}{\tau_b} \tag{B46}$$

If the restriction that the speed at any time $N(t)$ is always less than the final speed $N(t_1)$, then the right side of equation (B46) is negative and, for the same reason, the left side is positive. Therefore, it has been proved that the right hand side of equation (B44) is positive, so the left side of equation (B44) must always be positive under these restrictions. If the left side of equation (B44) is positive, there are two possibilities:

(1) If $\tau > \tau_b$, then $X(t_1) < 0$, which means that $T_b(t_1)$ will be greater than the steady-state value of blade temperature at t_1.

(2) If $\tau_b > \tau$, then $X(t_1) > 0$, which means the $T_b(t_1)$ is less than the steady-state value of blade temperature at time t_1.

REFERENCES

1. Ellerbrock, Herman H., Jr.: Some NACA Investigations of Heat-Transfer of Cooled Gas-Turbine Blades. Section V, Special Problems, General Discussion on Heat Transfer. Inst. Mech. Eng. and A.S.M.E. Conference (London), Sept. 11-13, 1951.

2. Brown, Gordon S., and Campbell, Donald P.: Principles of Servomechanisms. John Wiley and Sons, Inc., 1948.

3. LaVerne, Melvin E., and Boksenbom, Aaron S.: Frequency Response of Linear Systems from Transient Data. NACA Report 977, 1950. (Formerly NACA TN 1935.)

4. Feder, Melvin S., and Hood, Richard: Analysis for Control Application of Dynamic Characteristics of Turbojet Engine with Tail-Pipe Burning. NACA TN 2183, 1950.

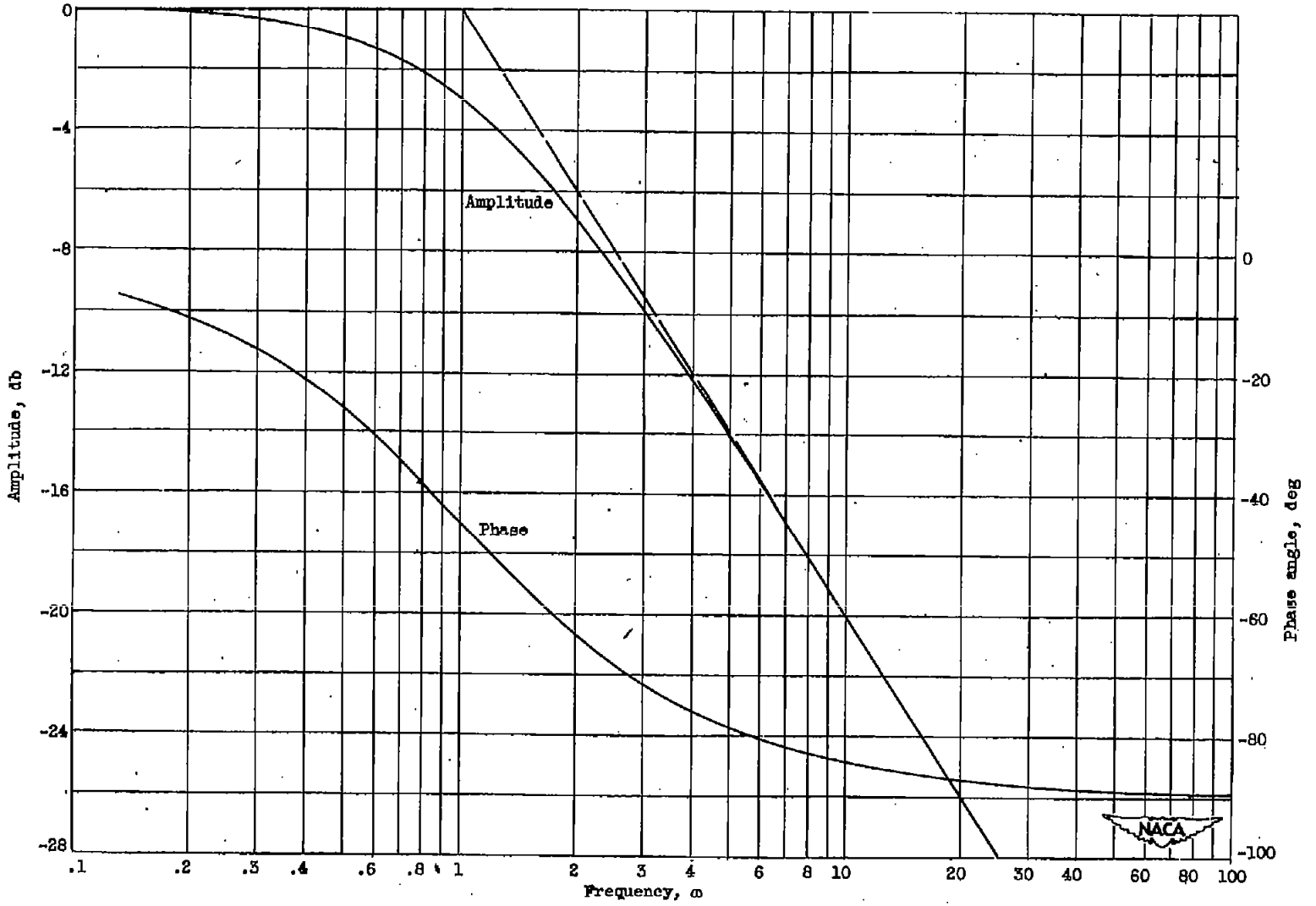

Figure 1. - Frequency response of turbine-blade temperature to gas temperature.

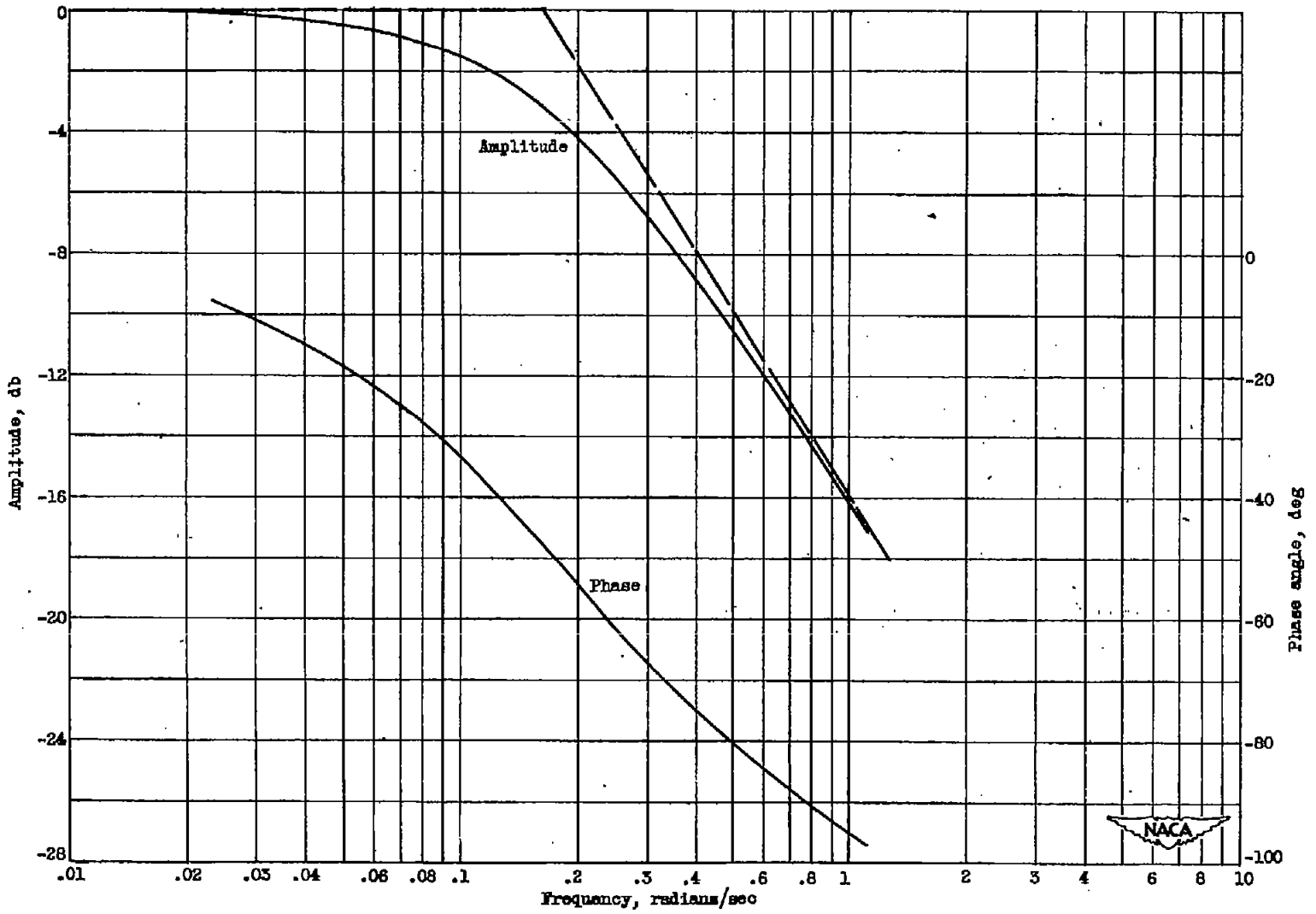

(a) Leading-edge blade temperature.

Figure 2. - Frequency response of turbine-blade temperature to gas temperature for analytical method B.

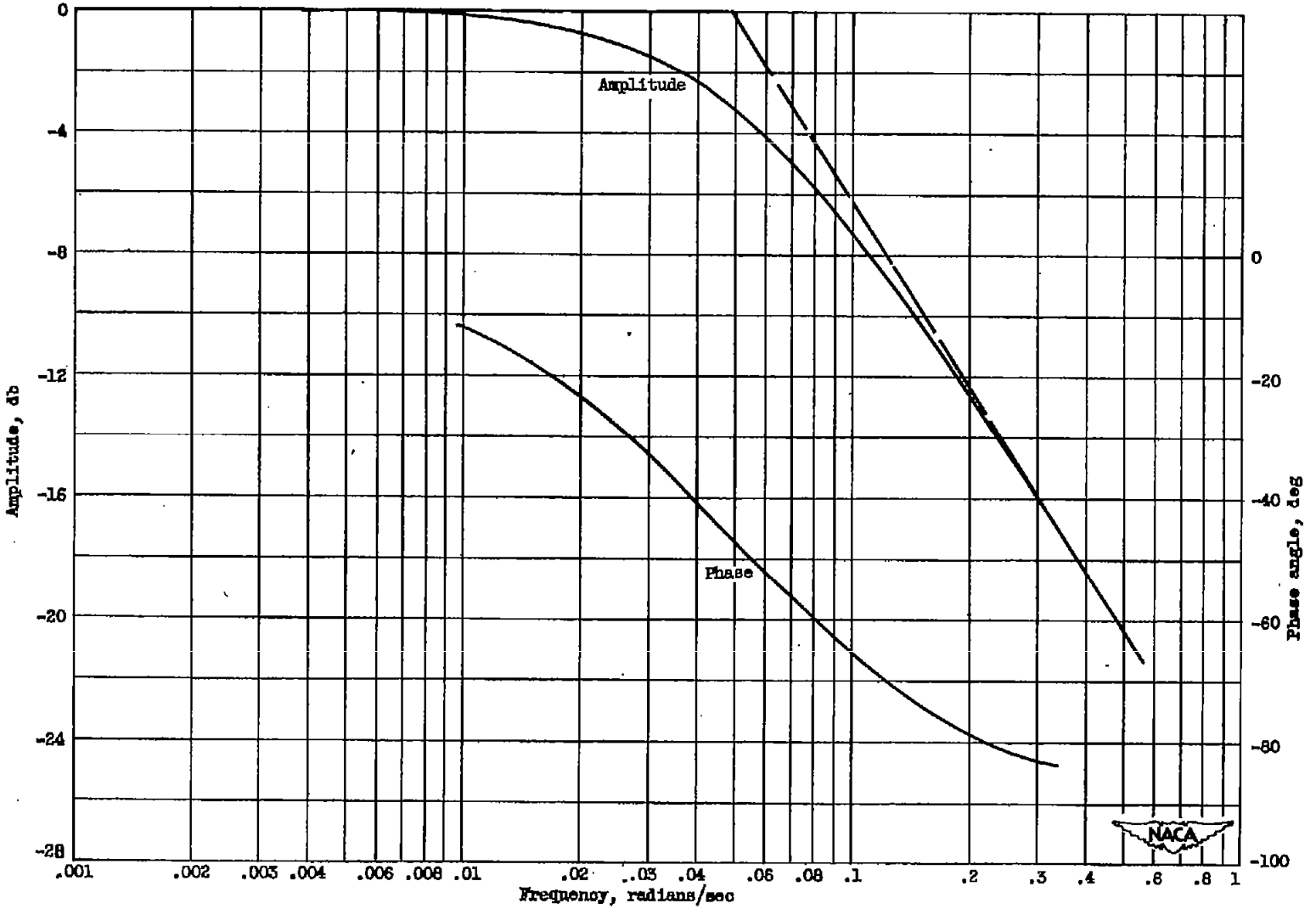

(b) Midchord blade temperature.

Figure 2. - Concluded. Frequency response of turbine-blade temperature to gas temperature for analytical method B.

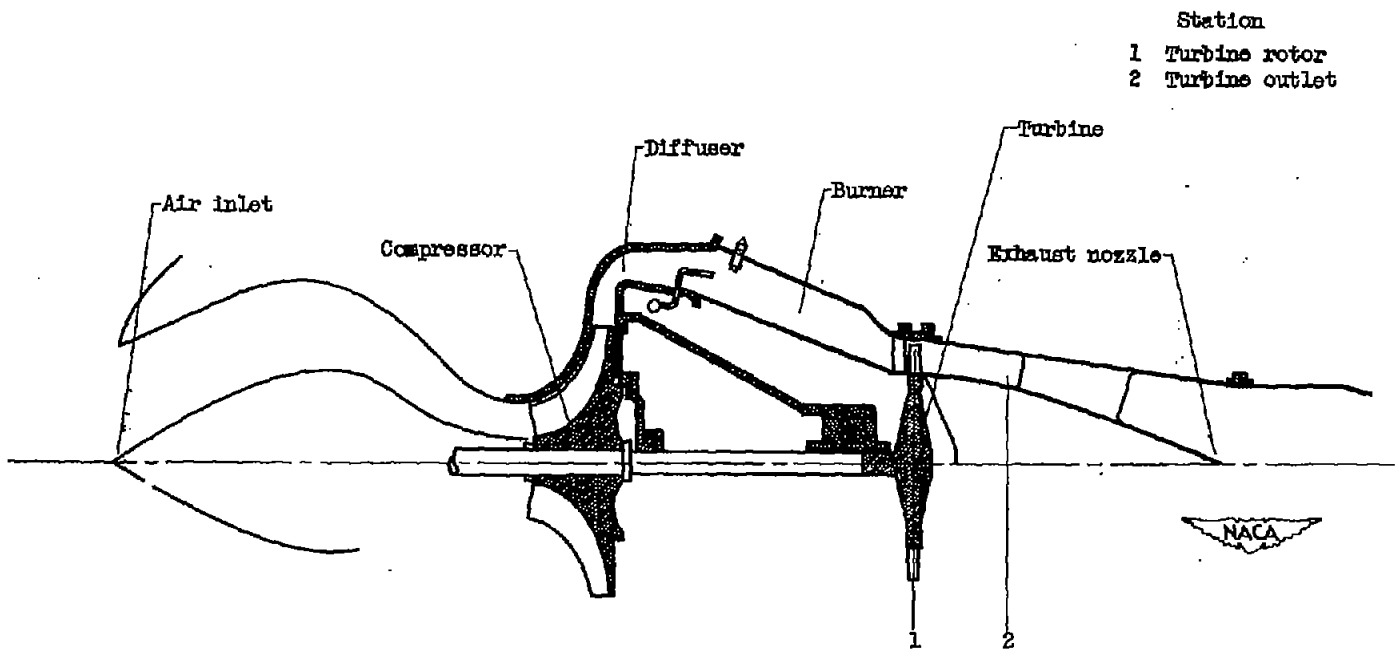

Figure 3. - Schematic drawing of turbojet engine.

CONFIDENTIAL

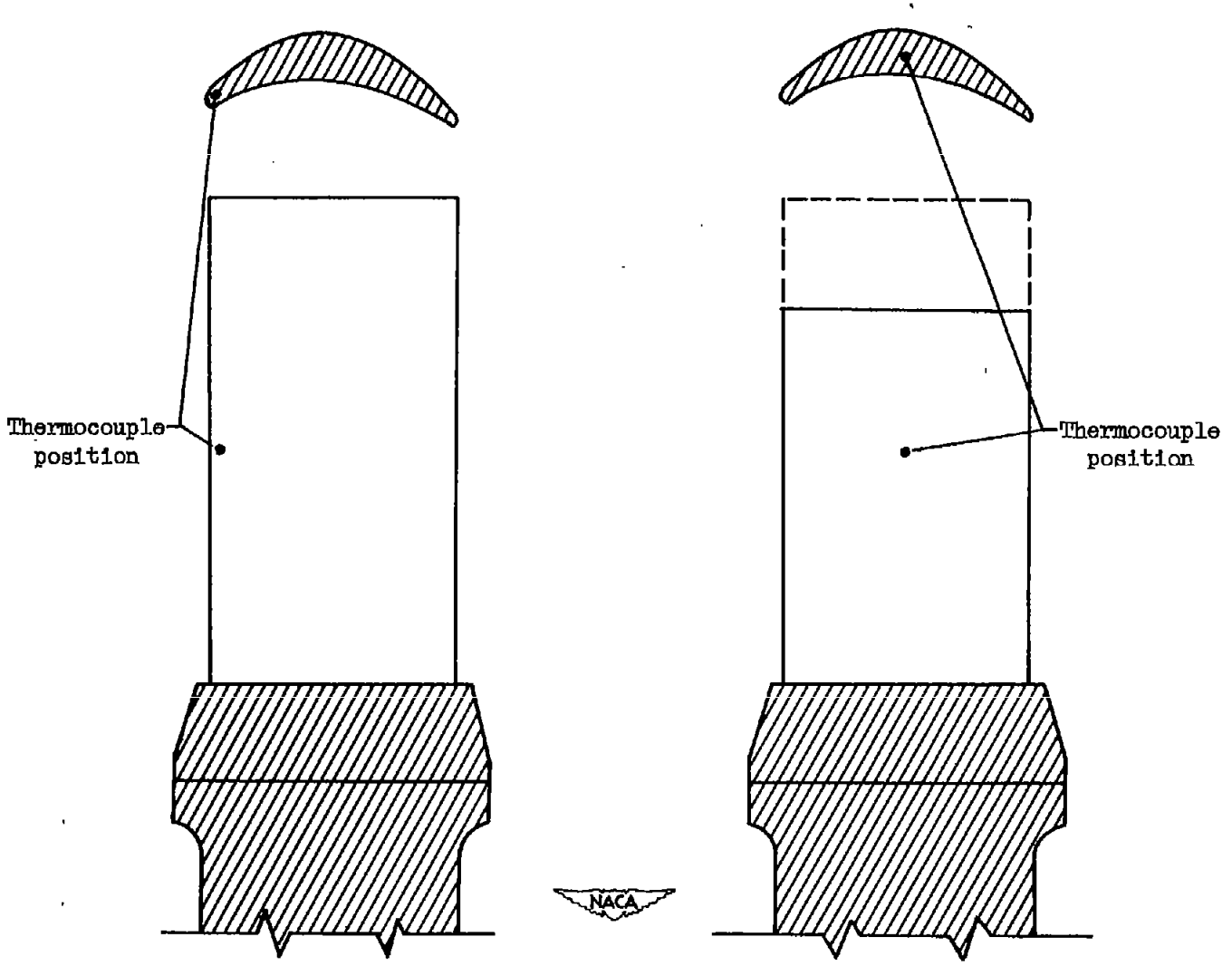

(a) Leading-edge position. (b) Midchord position.

Figure 4. - Turbine-blade thermocouple positions.

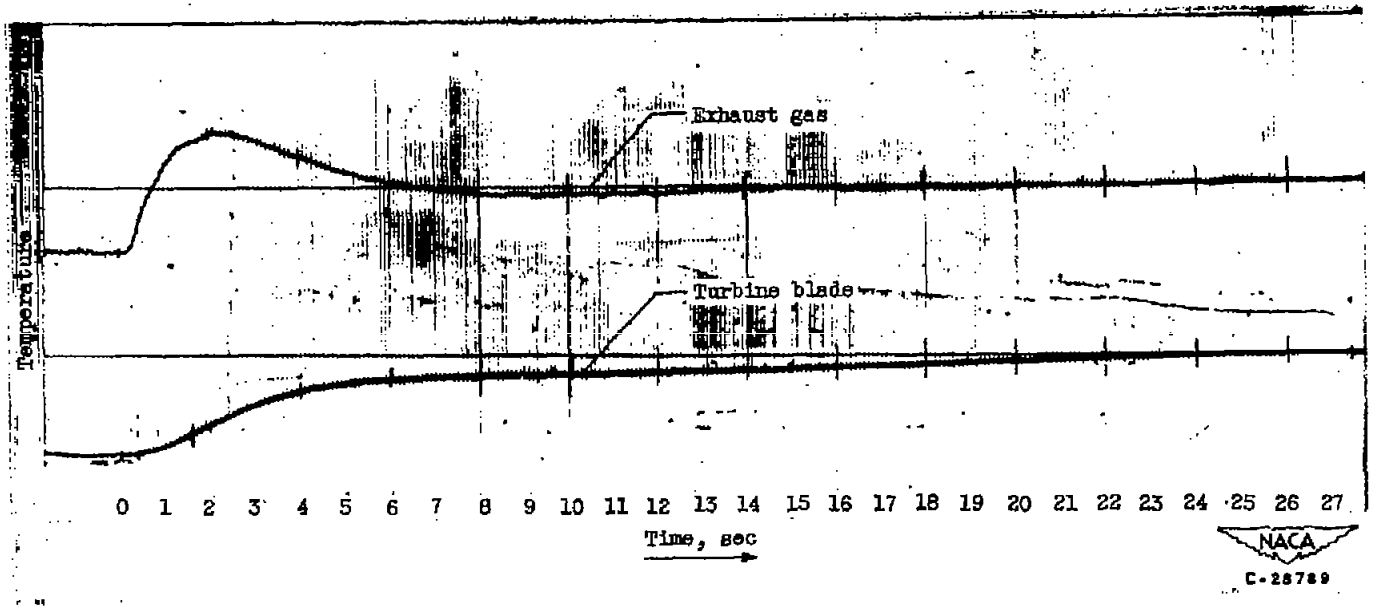

Figure 5. - Typical oscillograph traces for engine acceleration.

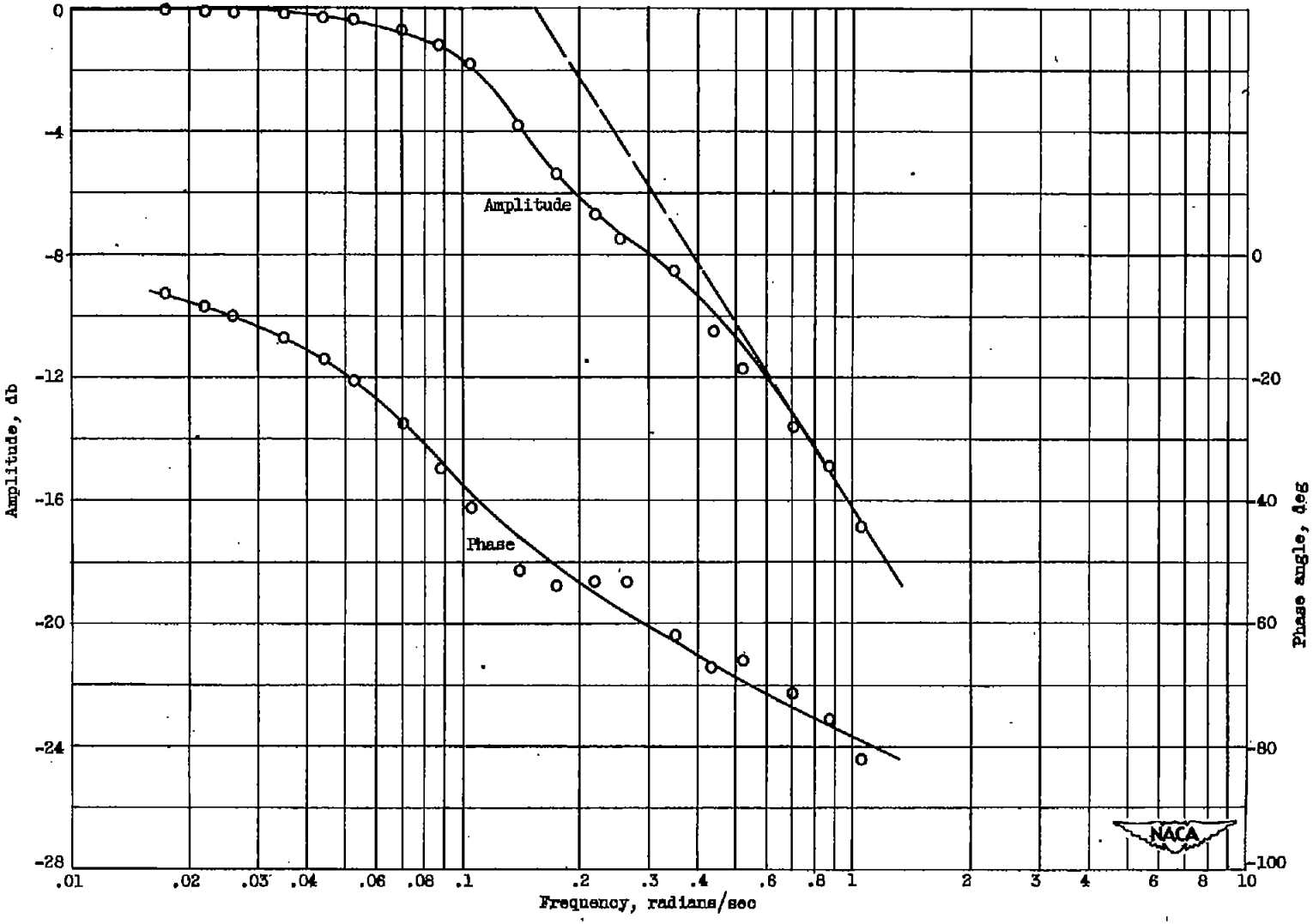

Figure 6. - Experimental frequency response of leading-edge blade temperature to gas temperature for engine acceleration.

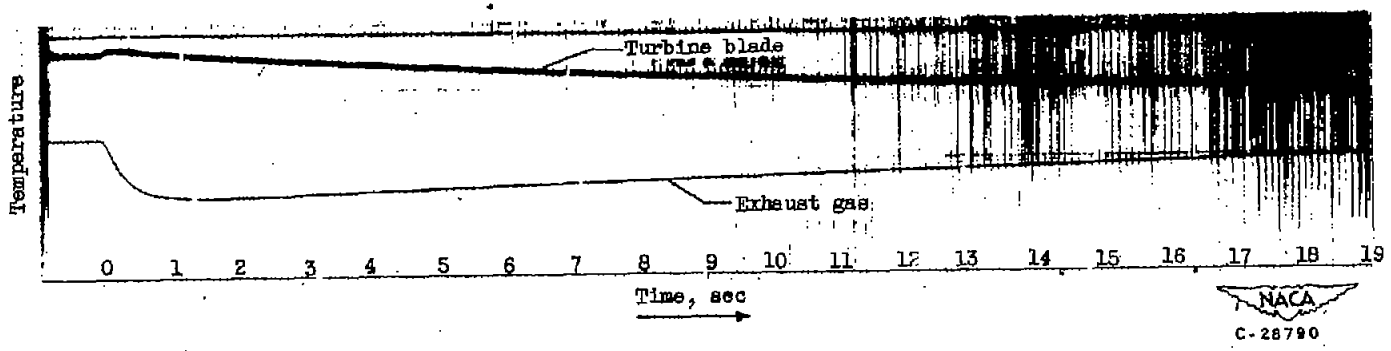

Figure 7. - Typical oscillograph traces of blade and gas temperature during a deceleration.

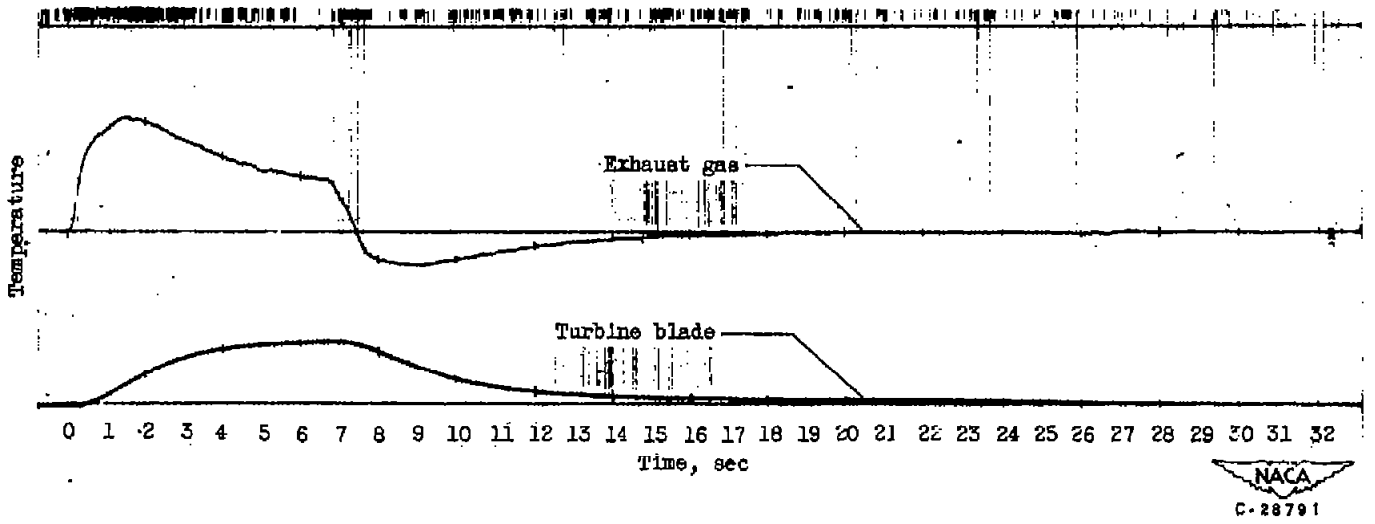

Figure 8. - Typical oscillograph traces of blade and gas temperature during acceleration followed by a deceleration.

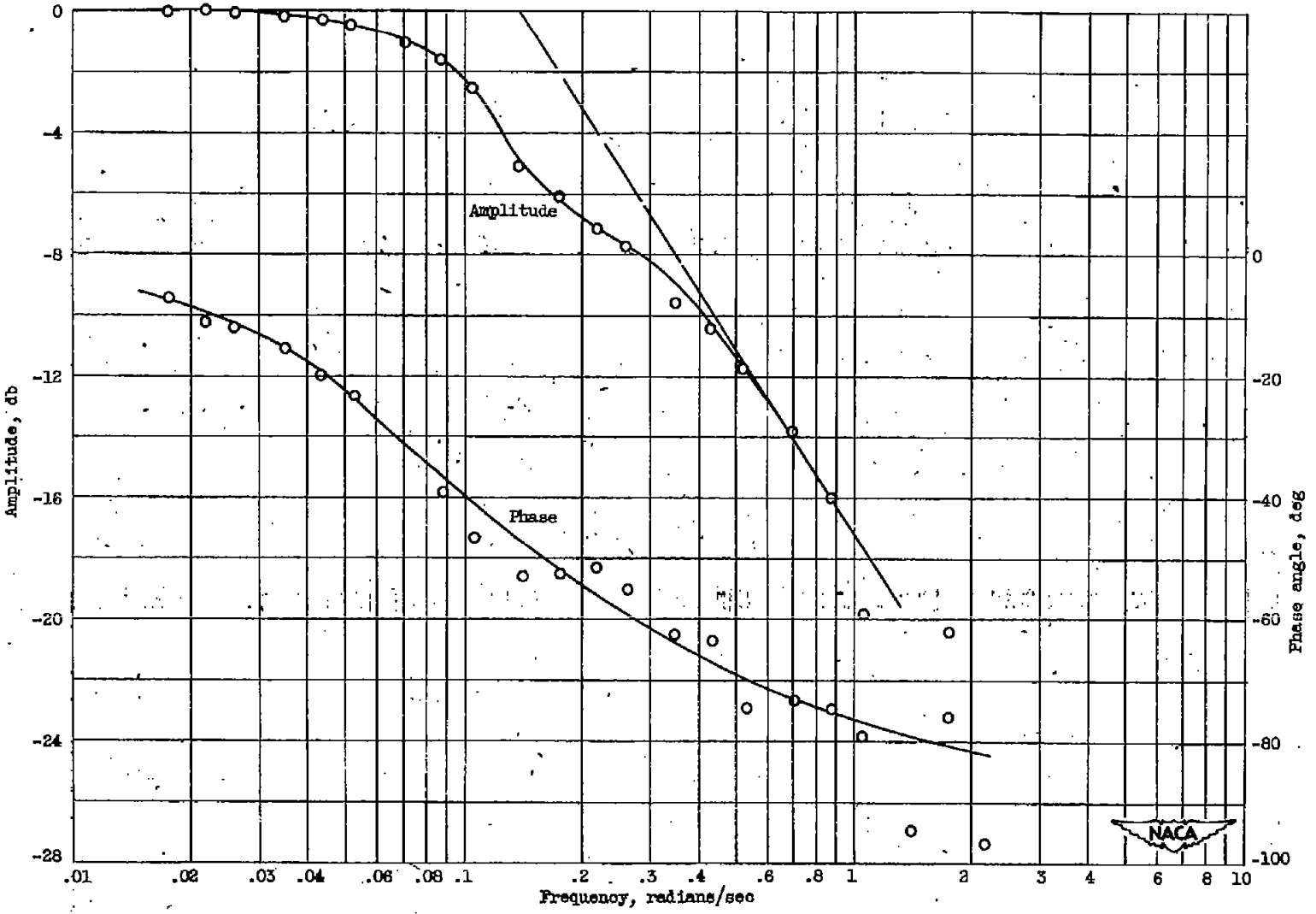

Figure 9. - Experimental frequency response of leading-edge blade temperature to gas temperature during an engine acceleration.

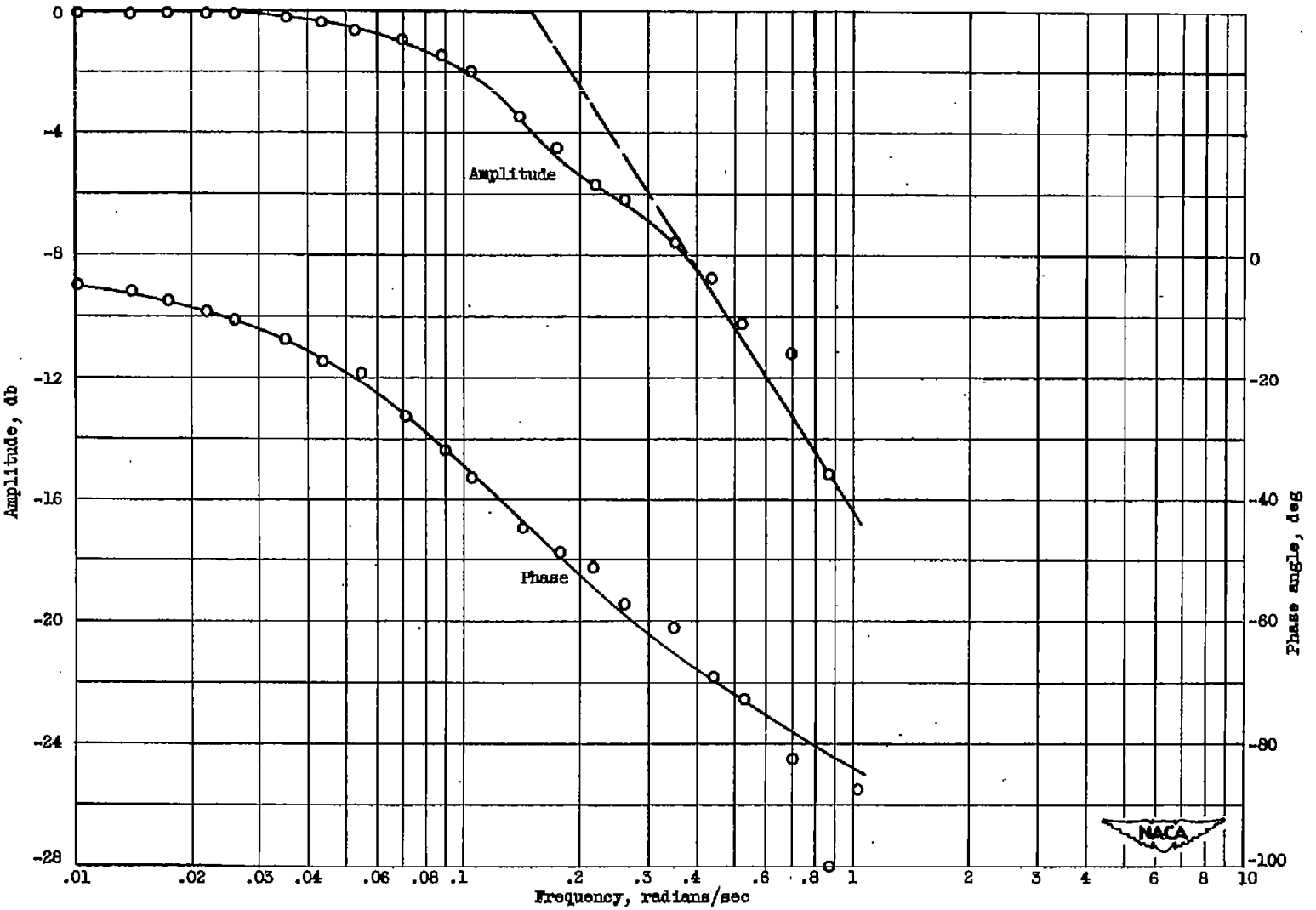

Figure 10. - Experimental frequency response of leading-edge blade temperature to gas temperature during an engine acceleration followed by a deceleration.

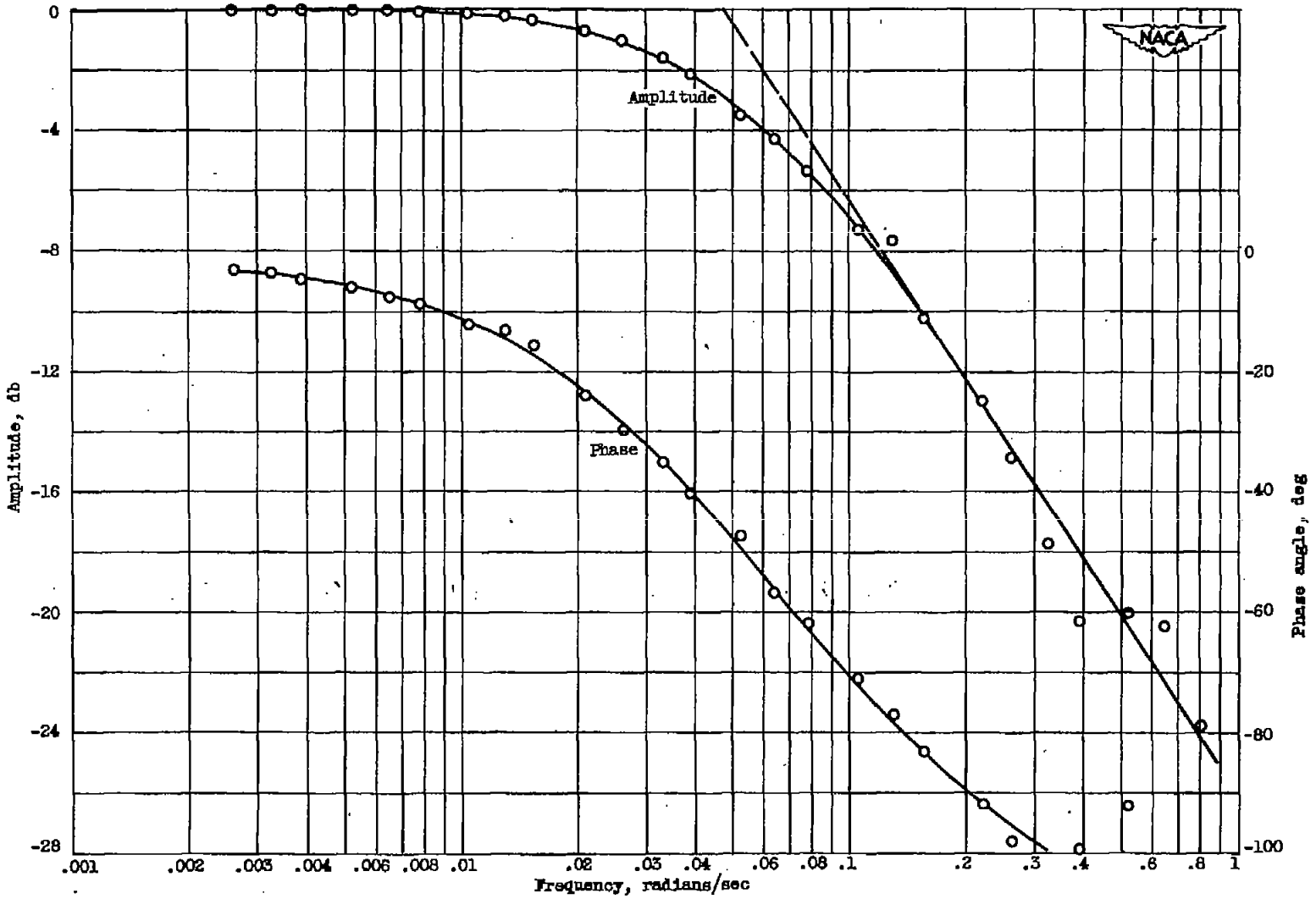

Figure 11. - Experimental frequency response of midchord blade temperature to gas temperature during an engine deceleration.

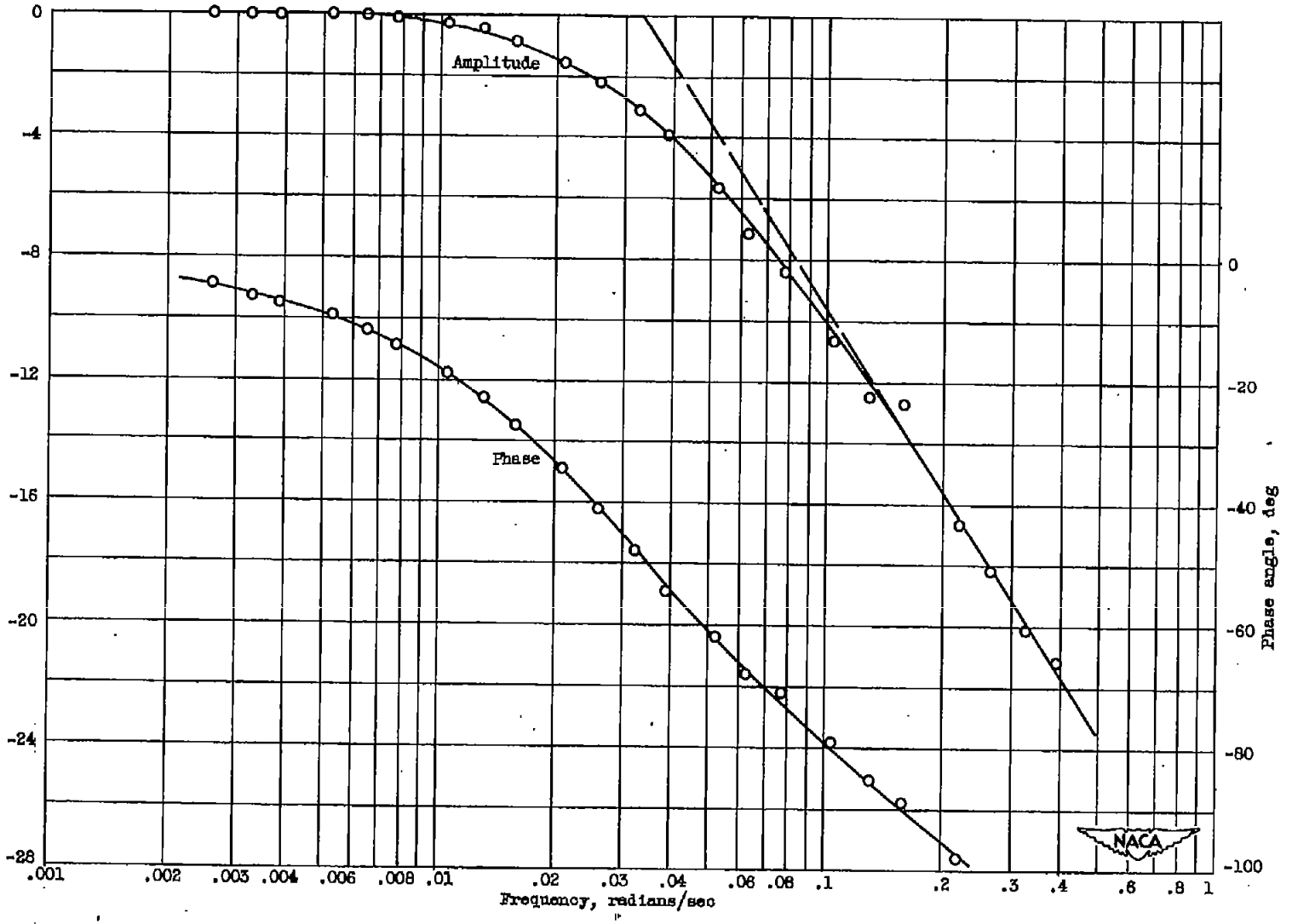

Figure 12. - Experimental frequency response of midchord blade temperature to gas temperature during an engine acceleration.

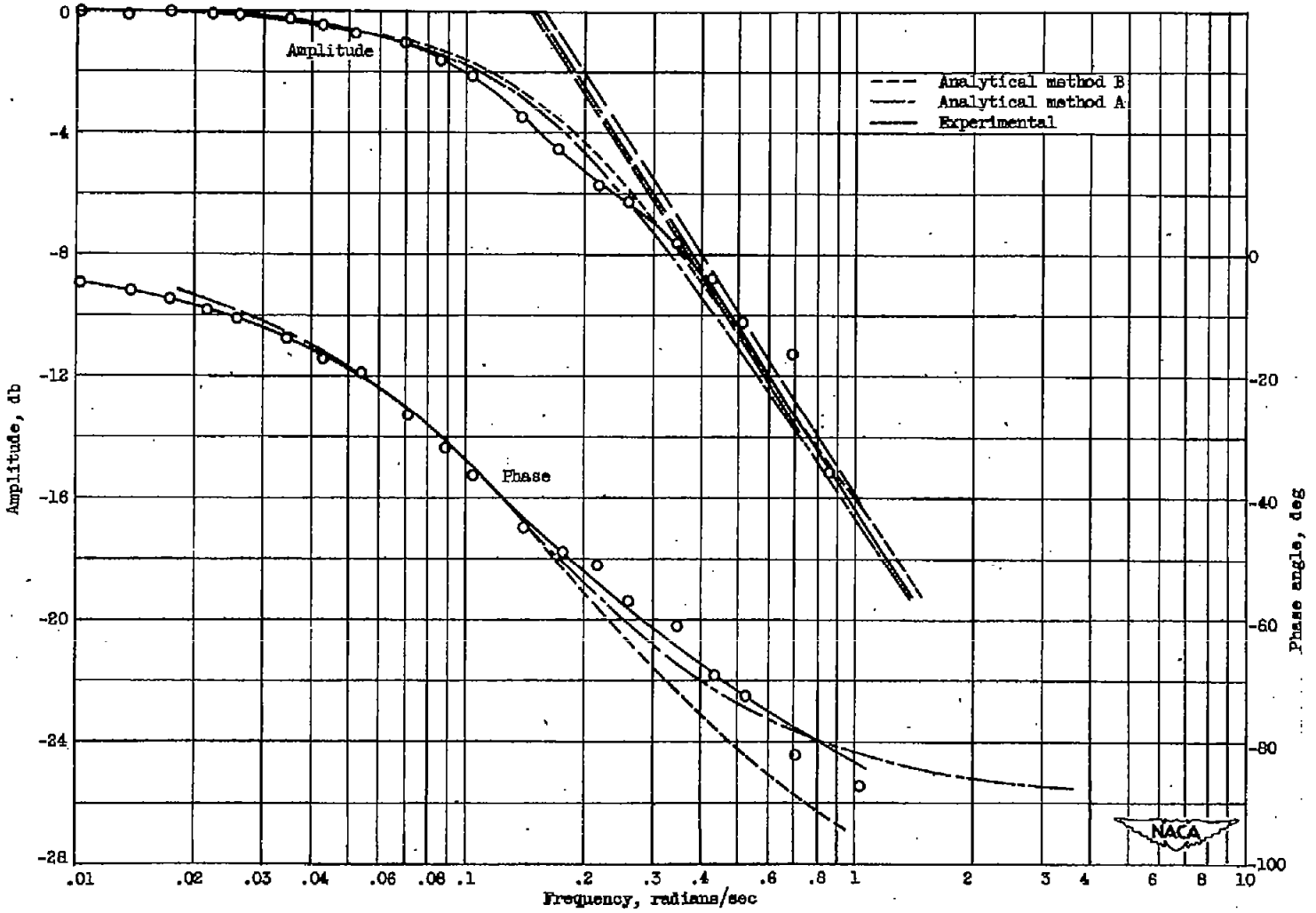

(a) Leading-edge blade temperature.

Figure 13. - Comparison of analytical and experimental frequency responses of blade temperature to gas temperature.

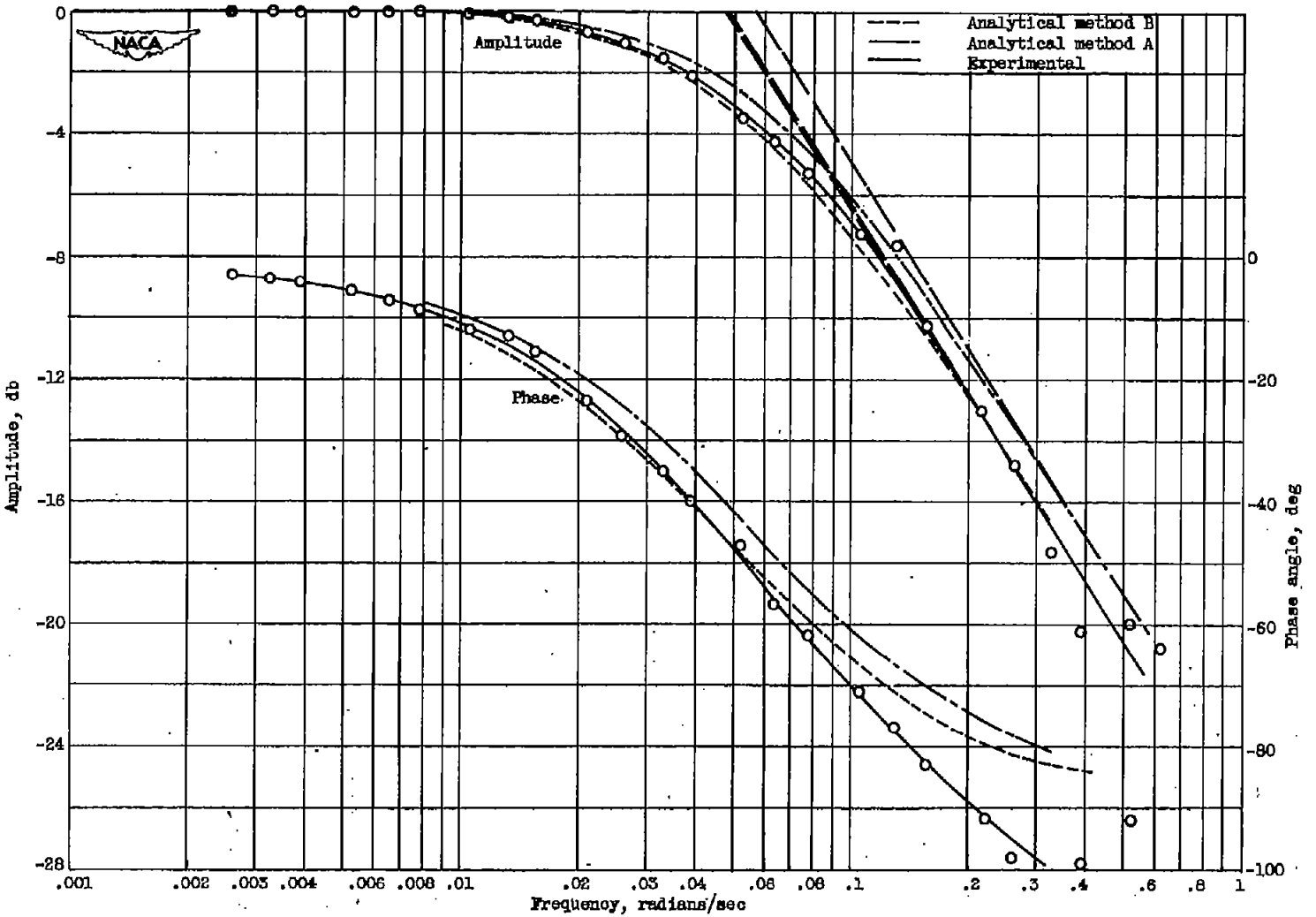

(b) Midchord blade temperature.

Figure 13. - Concluded. Comparison of analytical and experimental frequency responses of blade temperature to gas temperature.

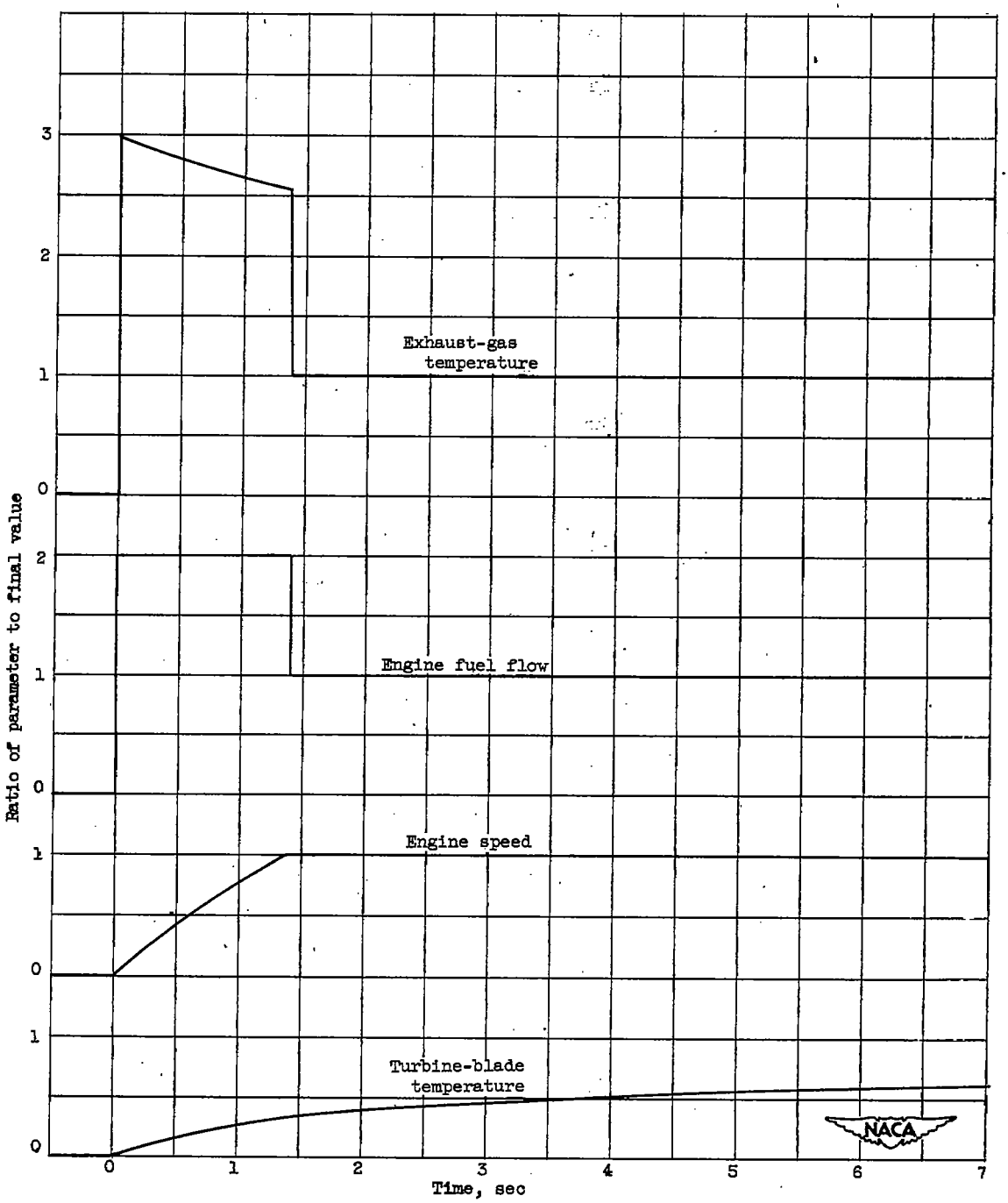

Figure 14. - Illustration of engine transient for turbine-blade time constant greater than engine time constant.

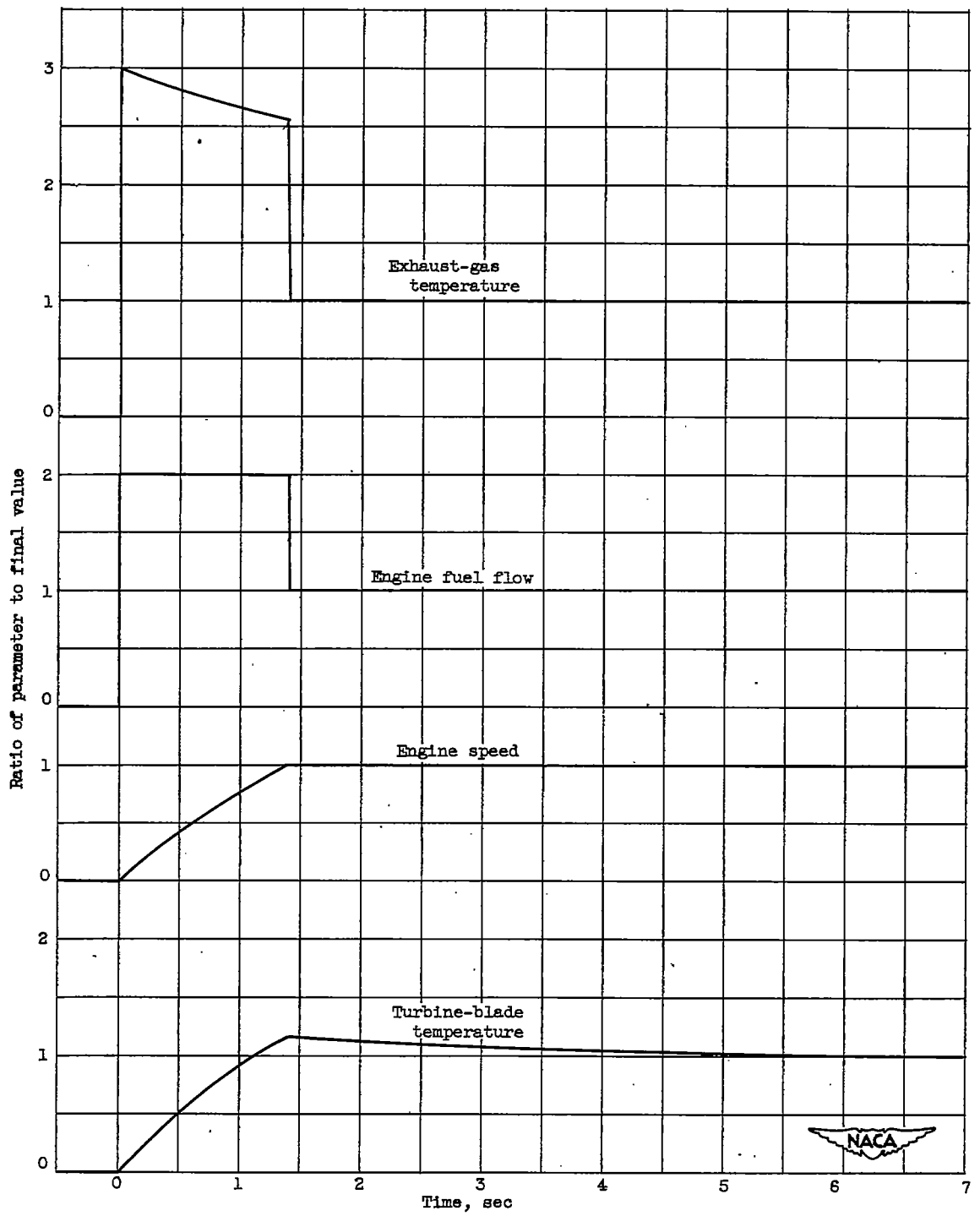

Figure 15. - Illustration of engine transient for turbine-blade time constant less than engine time constant.

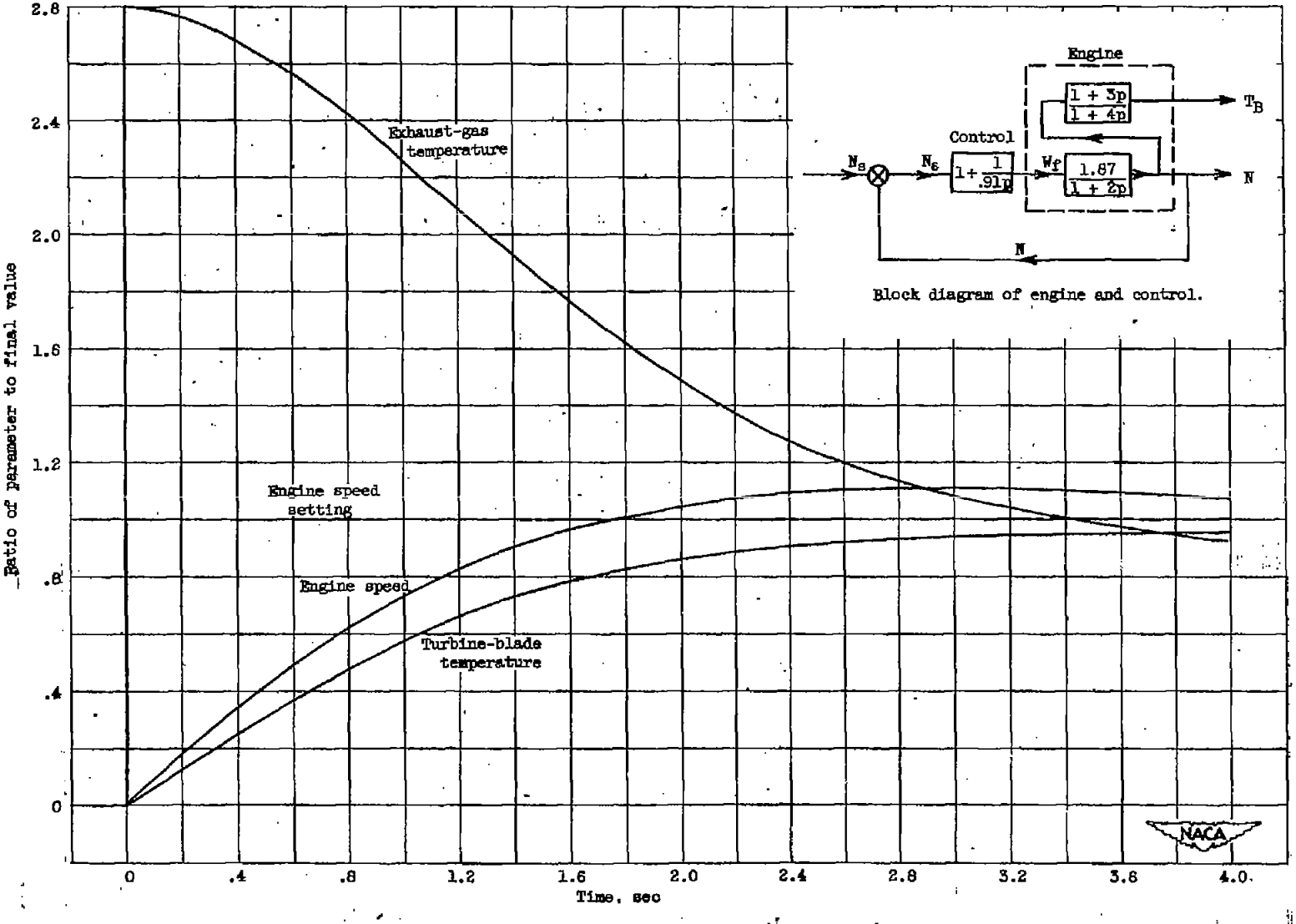

Block diagram of engine and control.

Figure 16. - Indicial response of speed setting to engine speed and temperatures of controlled turbojet engine.

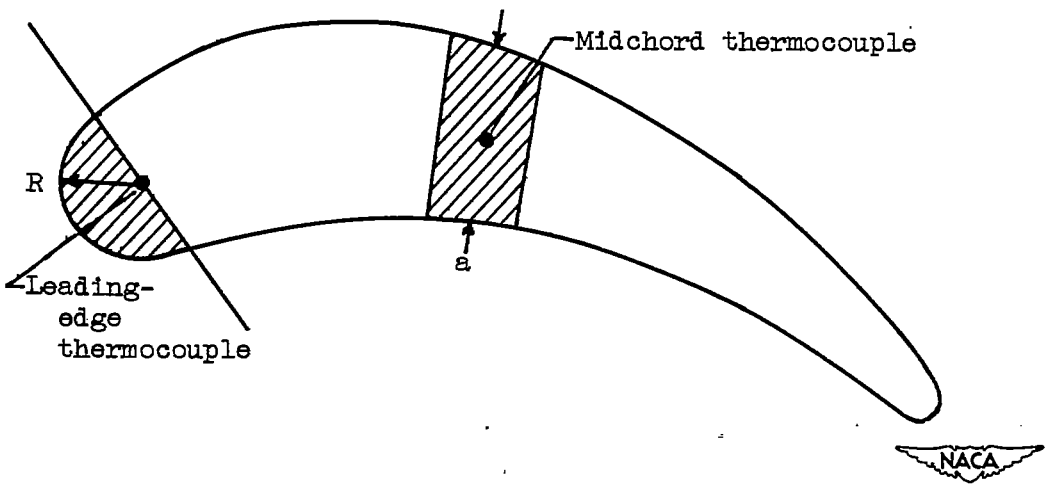

Figure 17. - Turbine-blade areas considered in analytical development of turbine-blade time constants.

NACA-Langley - 2-20-52 - 325